BioChip J. (2018) 12(4): 257-267
DOI 10.1007/s13206-018-2401-2

Review Article

Inertial Microfluidics-Based Cell Sorting

Ga-Yeong Kim[1], Jong-In Han[1] & Je-Kyun Park[2,*]

Received: 17 September, 2018 / Accepted: 22 November, 2018 / Published online: 07 December, 2018

Abstract Inertial microfluidics has attracted significant attention in recent years due to its superior benefits of high throughput, precise control, simplicity, and low cost. Many inertial microfluidic applications have been demonstrated for physiological sample processing, clinical diagnostics, and environmental monitoring and cleanup. In this review, we discuss the fundamental mechanisms and principles of inertial migration and Dean flow, which are the basis of inertial microfluidics, and provide basic scaling laws for designing the inertial microfluidic devices. This will allow end-users with diverse backgrounds to more easily take advantage of the inertial microfluidic technologies in a wide range of applications. A variety of recent applications are also classified according to the structure of the microchannel: straight channels and curved channels. Finally, several future perspectives of employing fluid inertia in microfluidic-based cell sorting are discussed. Inertial microfluidics is still expected to be promising in the near future with more novel designs using various shapes of cross section, sheath flows with different viscosities, or technologies that target micron and submicron bioparticles.

Keywords: Cell sorting, Dean flow, Inertial microfluidics, Inertial migration, Spiral channel, Straight channel

[1]Department of Civil and Environmental Engineering, Korea Advanced Institute of Science and Technology (KAIST), 291 Daehak-ro, Daejeon 34141, Republic of Korea
[2]Department of Bio and Brain Engineering, Korea Advanced Institute of Science and Technology (KAIST), 291 Daehak-ro, Daejeon 34141, Republic of Korea
*Correspondence and requests for materials should be addressed to J.-K. Park (✉jekyun@kaist.ac.kr)

Introduction

The ability of microfluidics to precisely manipulate the motion of particles on the microscale has been widely utilized for the three-dimensional focusing of various biological particles and the separation of microparticles or cells based on their unique biophysical properties such as size, shape, density, and surface proteins[1-4]. In particular, these cell sorting technologies can be used for a wide range of applications, such as single cell level detection and analysis for on-chip flow cytometry[5,6], preparation of biological samples[7-9] as well as isolation and enrichment of certain target cells[10,11].

To date, a number of cell sorting technologies have already been proposed, and these technologies can be divided into two categories, active and passive types, depending on whether an external force is used or not. The active technologies rely on the external force field, and they include dielectrophoresis[12,13], magnetophoresis[14-16], acoustophoresis[17-19], and optical tweezer[20,21]. On the other hand, passive types separate the cells without an externally applied force, and they are entirely dependent on the channel geometry or intrinsic hydrodynamic characteristics. Pinched flow fractionation[22,23], deterministic lateral displacement[24-26], hydrophoresis[27-29], and inertial microfluidics[30,31] belong to these passive types.

An active technology usually provides a more precise manipulation of target samples as well as being adjustable in real time. However, they often require expensive or complex external equipment, and the flow rate is limited since the externally applied force should overcome the hydrodynamic drag force to obtain high performance[2,32]. In contrast, the passive types are simple and working with a relatively high flow rate.

Among various passive microfluidic technologies, in-

ertial microfluidics has recently gained significant attention due to its high throughput, simplicity, and low cost[30,33-35]. In particular, it offers precise control of particles at high speeds of around 10^0–10^2 mL h^{-1} that could not have been achieved with the traditional cell sorting technologies (10^{-4}–10^0 mL h^{-1}) (Figure 1).

This inertial microfluidics is also characterized by their relatively high Reynolds numbers (Re) between ~1 and ~100[30]. Re is the ratio of inertial force to viscous force, which can be defined as:

$$\mathrm{Re} = \frac{\rho U H}{\mu} \quad (1)$$

where ρ, U, H, and μ are the density of fluid, average flow velocity, characteristic channel dimension, and dynamic viscosity, respectively. In most microfluidic applications, Re takes a value below 1 (Stokes regime, Re $\rightarrow$0), where the denominator, viscous force, is dominant, and the numerator, fluid inertia, is negligible. However, there is an intermediate regime (~1 < Re < ~100) between this Stokes regime and turbulent regime (Re > ~2000), where the inertial forces are no longer negligible, and both inertia and viscosity of the fluid become finite[31]. In this inertial microfluidics regime, the flow is still laminar, but the inertial forces affect the movement of the particles, enabling the particle sorting.

In detail, this finite inertia of the fluid brings two intriguing phenomena of (i) inertial migration and (ii) Dean flow (secondary flow), and the geometry of microfluidic channels is the most critical parameter that determines the effect of these two phenomena as well as the functionality of the entire microfluidic devices[31]. In this regard, the inertial microfluidics-based devices can be broadly classified into (i) straight channels and (ii) spi-

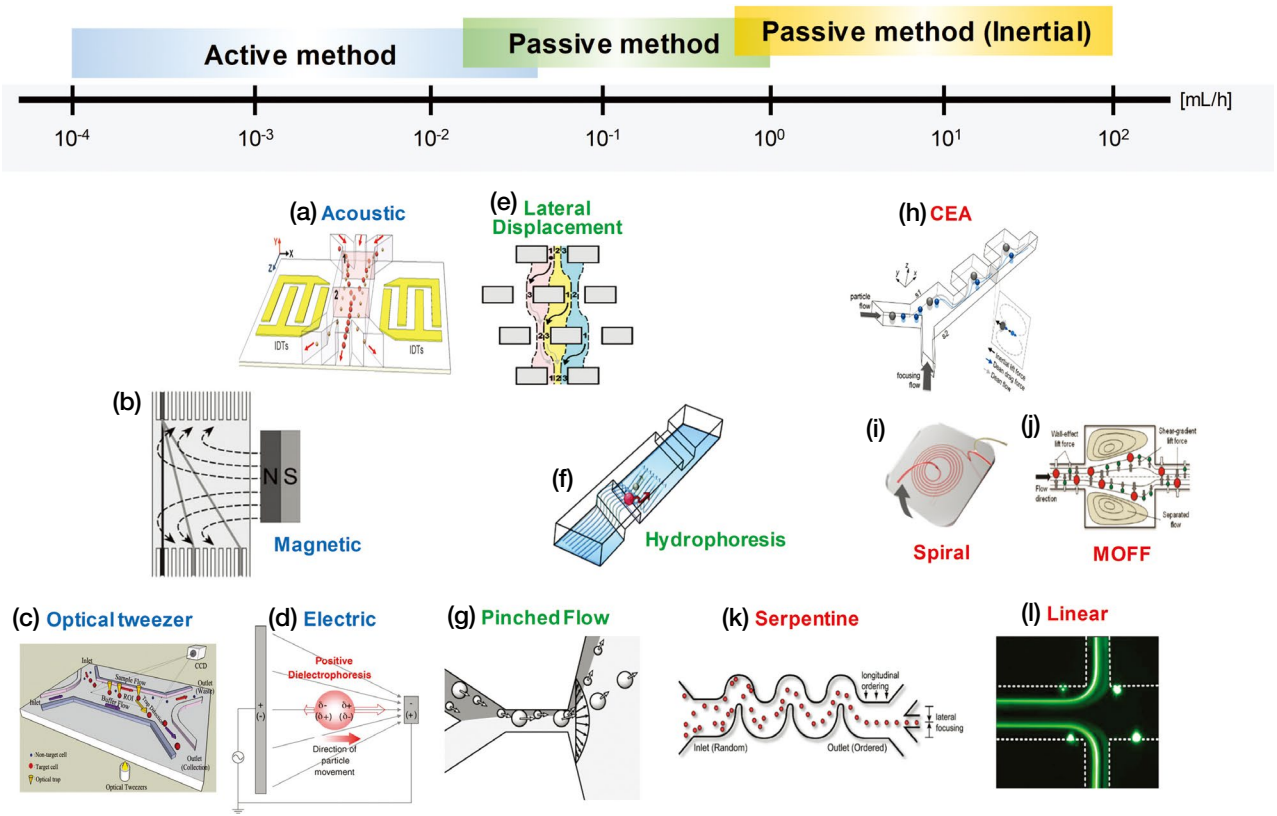

Figure 1. Comparison of the separation throughput between active and passive methods of cell sorting. (a) Acoustic. Reproduced with permissions[17]. Copyright 2009, Royal Society of Chemistry; (b) Magnetic. Reproduced with permissions[14]. Copyright 2007, Royal Society of Chemistry; (c) Optical tweezer. Reproduced with permissions[20]. Copyright 2011, Royal Society of Chemistry; (d) Electric. Reproduced with permissions[12]. Copyright 2005, Elsevier; (e) Lateral displacement. Reproduced with permissions[24]. Copyright 2004, The American Association for the Advancement of Science; (f) Hydrophoresis. Reproduced with permissions[27]. Copyright 2007, Royal Society of Chemistry; (g) Pinched flow. Reproduced with permissions[22]. Copyright 2004, American Chemical Society; (h) Contraction–expansion array (CEA). Reproduced with permissions[36]. Copyright 2011, Elsevier; (i) Spiral. Reproduced with permissions[37]. Copyright 2018, American Chemical Society; (j) Multiorifice flow fractionation (MOFF). Reproduced with permissions[38]. Copyright 2009, American Chemical Society; (k) Serpentine. Reproduced with permissions[33]. Copyright 2007, National Academy of Sciences; (l) Linear. Reproduced with permissions[34]. Copyright 2008, AIP Publishing.

ral channels depending on their channel structure.

In this review, the basic principles of inertial migration and Dean flow in these two representative structured microchannels are first explained, and the current progress and various applications of inertial microfluidics are then discussed. Finally, several future perspectives on microfluidic-based cell sorting are introduced.

Inertial Migration in Straight Channels

Theoretical Backgrounds

Inertial migration is the phenomenon that the randomly distributed particles entering a straight channel move laterally to their specific designated equilibrium positions[31,39,40], and this inertial migration is caused by the sum of two forces, the shear-induced lift force ($\mathbf{F}_{LS}$) and wall-induced lift force ($\mathbf{F}_{LW}$) (Figure 2).

In a straight channel, because of the curvature of the fluid velocity profile, a particle in a maximum of the parabola (channel centerline) experiences a larger relative velocity than a particle near the wall. This difference in velocity induces a force, $\mathbf{F}_{LS}$, which drives the particles out from the channel centerline. This shear-induced lift force competes with another lift force, the wall-induced lift force, which is formed as a result of inertia of the fluid around the particle when the particles migrate closer to the walls[41]. This wall-induced lift force pushes the particles away from the walls, directing the particle in the opposite direction to the shear-induced lift force. Therefore, the point at which these two forces, $\mathbf{F}_{LS}$ and $\mathbf{F}_{LW}$, are balanced becomes the inertial equilibrium position of a particle, and the net inertial lift force ($\mathbf{F}_L$) and the lateral migration velocity of particle (U_L) can be expressed as:

$$\mathbf{F}_L = \frac{f_L \rho U^2 a^4}{H^2} \tag{2}$$

$$U_L = \frac{\mathbf{F}_L}{3\pi\mu a} = \frac{\rho U^2 a^3}{6\pi\mu H^2} \tag{3}$$

where f_L is the lift coefficient, and a is the diameter of particle[30]. The biquadratic dependence of this net inertial lift force on the particle size ($\mathbf{F}_L \propto a^4$) causes the particles to have different equilibrium positions according to their sizes.

There are several criteria that are used to determine whether a given microfluidic channel is appropriate to inertially sort the particles[35], and the efficiency of inertia-based separation depends on various hydraulic and geometrical parameters. First, there is a theoretical minimum channel length required (L_{min}) for the particles to reach their stable inertial equilibrium positions, and in

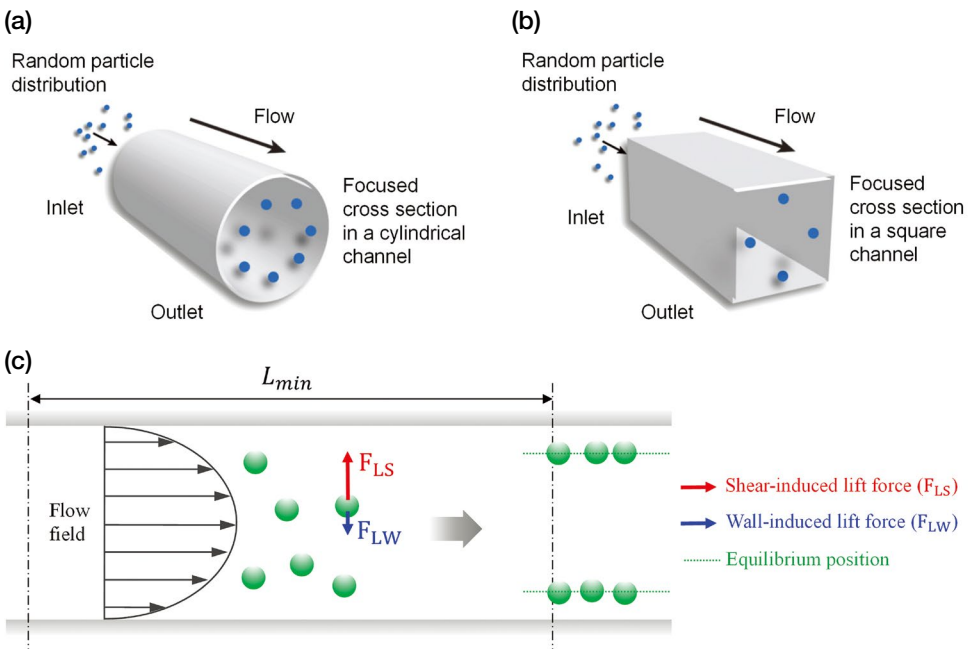

Figure 2. Inertial migration in a straight channel. (a) Inertial migration in a cylindrical channel. Redrawn with permissions[30]. Copyright 2009, Royal Society of Chemistry. (b) Inertial migration in a square channel. Redrawn with permissions[30]. Copyright 2009, Royal Society of Chemistry. (c) The shear-induced lift force ($\mathbf{F}_{LS}$) arises from the curvature of the velocity profile, while the wall-induced lift force ($\mathbf{F}_{LW}$) arises from the wall repulsion.

order to obtain high resolution with clear separation, enough channel length longer than L_{min} should be provided in a practical experimental setting.

$$L_{min} \approx \frac{H}{2U_L} \times U = \frac{3\pi\mu H^3}{\rho U a^3} \quad (4)$$

The second rule covers the particle Reynolds number (Re_P), which is related to the ratio of particle size (a) to channel size (H).

$$Re_P = Re\frac{a^2}{H^2} = \frac{\rho U a^2}{\mu H} \quad (5)$$

When Re_P is in the order of 1, the inertial lift forces and lateral migration of particles across the fluid streamlines are reported to become dominant[31]. It has also been empirically proven that the ratio of $a/H > 0.07$ is required to capitalize on the inertial effects[33]. This implies that only the particles that are large with respect to the channel dimensions have inertial effects. Hence, it is necessary to carefully control these parameters, a, H, U, L_{min}, for the fixed ρ, μ of the fluid.

Applications of Straight Channels

The straight channels have been often used to investigate the basic principles of inertial migration and have also been utilized for various applications. As an example, the separation of pathogenic bacteria from diluted blood samples was demonstrated in a simple straight channel, which is composed of short focusing, gradual expansion, and collection region (Figure 3a)[41]. Initially, randomly dispersed red blood cells at the inlet of the channel are arranged into two aligned streams by inertial lift force. While passing through the next gradual expansion region, these equilibrium positions are shifted closer to the wall, increasing the extraction and concentration efficiency. After two passes of this single channel system, >80% of the pathogens were removed.

This straight channel can also be applied to isolate the cell-laden hydrogel droplets from empty droplets (Figure 3b)[42]. Hydrogel droplets containing microalgae of *Euglena gracilis*, shrink as the cells grow and divide, whereas the empty hydrogel droplets retain their size. In a straight channel, larger empty droplets are focused closer to the channel centerline compared to the smaller algae droplets. With this principle, this study collected the *Euglena gracilis*-laden droplets with a purity of up to 93.6%, and an enrichment factor of up to 5.51 without significantly affecting the cell viability.

In addition, a cascaded channel consisting of two straight segments with different aspect ratios allows more precise separation (Figure 3c)[43]. Randomly distributed particles flowing through a high aspect ratio segment are first focused near the two sidewalls, and then these equilibrium positions are modified to near the channel centerline as the channel expands into a low aspect ratio segment. Because the larger particles have a much higher lateral migration velocity ($U_L \propto a^3$), they reach the new equilibrium points more quickly. On the contrary, the inertial lift forces acting on the smaller particles are not strong enough to drag them into the channel centerline. The particles, thus, can be separated more clearly by employing these different aspect ratios. In this study, a complete isolation of rare human prostate epithelial tumor cells from blood was successfully demonstrated.

Godino *et al*. also adopted this straight channel to prevent the invasion of undesired species during the cultivation process. For instance, the quantity and quality of

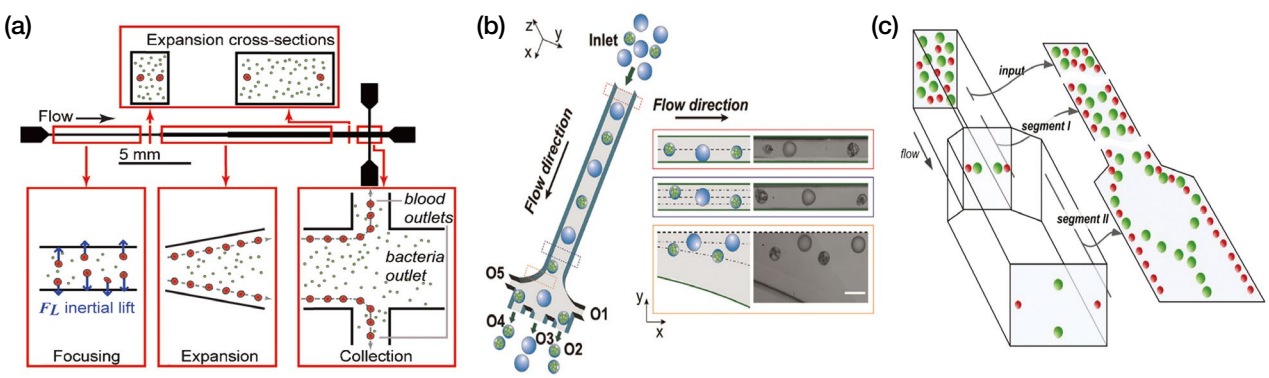

Figure 3. Various applications utilizing straight channels. (a) Separation of pathogenic bacteria from diluted blood samples. Reproduced with permissions[41]. Copyright 2010, John Wiley and Sons. (b) Isolation of the *Euglena gracilis*-laden hydrogel droplets from empty hydrogel droplets. Reproduced with permissions[42]. Copyright 2018, Royal Society of Chemistry. (c) A cascaded channel consisting of two straight segments with different aspect ratios to separate the human prostate epithelial tumor cells. Reproduced with permissions[43]. Copyright 2013, Royal Society of Chemistry.

microalgal products are often decreased by the contamination from the bacteria or other microalgae species, requiring laborious purification procedures. They conducted a straight channel-based separation of microalgae (10-30 μm) from the contaminating bacteria (1-2 μm) with an efficiency of $>99\%$[32].

In particular, this straight channel also has an effect of exchanging the medium[44-46]. When the particle suspension is injected from the two side inlets, and the fresh medium is infused from the central inlet, the old medium of particle suspension can be exchanged through the lateral migration of particles from the original side stream to the middle stream.

The straight channels are generally simple, and easy to operate; however, the sizes of channel cross sections are generally limited to provide sufficient inertial effects because the net inertial lift force is inversely proportional to the size of channel cross sections ($\mathbf{F}_L \propto H^{-2}$). Besides, a relatively long channel length is required, which would consequently result in a large device footprint. These weaknesses can be improved by the introduction of a secondary flow, which is caused by the channel curvature or obstacle structure.

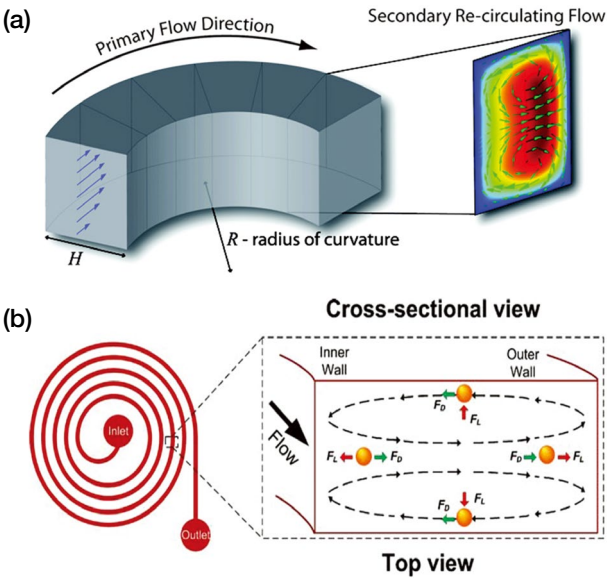

Figure 4. Dean flow (secondary flow) with two counter-rotating vortices in a curved channel. (a) Secondary re-circulating flow. Reproduced with permissions[30]. Copyright 2009, Royal Society of Chemistry. (b) Combination of inertial lift force and Dean drag force. Reproduced with permissions[48]. Copyright 2009, Springer Nature. $\mathbf{F}_L$: inertial lift force, $\mathbf{F}_D$: Dean drag force.

Inertial Migration in Curved Channels

Theoretical Backgrounds

When a curved structure is introduced into the channel (e.g., spiral channel), another flow, referred to as secondary flow or Dean flow, appears. This additional flow is formed by a pressure gradient in the radial direction due to the centrifugal force. The fluid elements near the channel centerline have a higher momentum than those near the wall[47]; hence, they tend to flow outward around a curve and cause relatively stagnant fluid elements near the channel wall to flow inward along the circumference[31], forming two counter-rotating streams, called Dean vortex (Figure 4)[30,48]. This Dean flow brings several benefits. It allows the particles to migrate to their equilibrium position more quickly with higher separation efficiency due to its mixing effects, and also leads to a reduction of the channel length and the overall device footprint.

The additional Dean flow also affects the migration of particles. The particles flowing through a curved channel with the Re between ~1 and ~100 experience both inertial lift forces and Dean drag force, so the effects of these two forces are superimposed on the particles in the spiral channels. The order of magnitude scaling between inertial lift forces and Dean drag force determines the final behavior of the suspended particles in the curved channel, and this is predicted by a dimensionless parameter, R_f, which is denoted as:

$$R_f = \frac{a^3 R}{H^3} \quad (6)$$

where R is the radius of curvature[31]. The dependency of R_f on the particle size ($R_f \propto a^3$) implies that it is possible to separate the particles according to their size even in the curved channels.

In detail, when R_f approaches 0, the Dean drag force governs the behavior of particles, and the inertial force is negligible. As a result, the particles remain entrained within the Dean flow streamlines. On the contrary, when R_f approaches infinite, the inertial lift force dominates over the Dean drag force; thus, the particles are aligned to their inertial equilibrium positions regardless of the Dean flow. In most cases with the intermediate range of R_f, however, the inertial equilibrium positions are modified by the Dean flow, resulting in new equilibrium points.

Similar to the curvature, the introduction of disturbance obstacles also induces local secondary rotating flows. The contraction–expansion array is one of the representative examples, and the contraction region acts as a curved structure[36,49-51]. As the fluids pass through the contraction region, the direction of the entering fluids is perpendicular to the direction of the main flow. This induces a local secondary flow and a

drag force ($\mathbf{F}_D$):

$$\mathbf{F}_D = 3\pi\mu U_{VW} a \quad (7)$$

where U_{VW} is the transverse velocity of secondary flow[52]. This Dean-like secondary flow only appears within the contracted channel, so that its effect on particle inertial focusing is intermittent[53]. As shown in Figure 5a, the direction of this Dean drag force is opposite to the net inertial lift fore. Since the net inertial lift force has much greater effect on the large particles due to its a^4 term ($\mathbf{F}_L \propto a^4$), the larger particles or cells migrate towards side 1 (s1) faster than the smaller particles or cells, and the Dean drag force causes the smaller particles or cells to move further to side 2 (s2)[50]. As the fluids continue to flow through the following contraction regions, the spatial distance between the particles' streamlines becomes clear, leading to a greater separation resolution. In addition, by changing the length of a contraction channel, the lateral migration of the desired particles or cells can be modulated to increase the separation (Figure 5b)[51]. With the extended contraction region, the large particles can be exposed to the inertial lift forces for a longer period of time, resulting in farther migration toward s1. On the contrary, small particles that are dominantly influenced by Dean drag force remain in similar lateral positions due to the fixed magnitude of the Dean-like secondary flow.

Applications of Curved Channels

The spiral channels can basically be used for the passive separation and sorting of particles. Kuntaegowdanahalli *et al*. demonstrated the continuous separation of three polystyrene beads with different diameters (10, 15, and 20 μm)[52]. They showed 90% of the high separation efficiency. In addition, a sheath-less, on-chip flow cytometry system was suggested[48]. The cells aligned by the spiral channel were detected and counted by the downstream laser-induced fluorescence setup. This system was found to have a high throughput of 2,100 particles per second.

This spiral type was also effective for the separation and enrichment of extremely rare circulating tumor cells (CTCs) from the blood sample. The device, called as "Dean Flow Fractionation", enabled the CTCs to be isolated from the blood samples of patients with advanced metastatic non-small cell lung cancer, achieving >85% of recovery[54]. The next generation spiral channel device with a trapezoidal cross section could achieve a higher separation resolution than the typical rectangular one (Figure 6a)[55]. The asymmetry of the trapezoidal cross section resulted in the formation of Dean vortex cores skewed towards the outer wall. This modified velocity field made the smaller platelets and white blood cells trapped inside the Dean vortex, unlike they were focused near the center of the channel width in the traditional rectangular channels. With the relatively larger CTCs focused closer to the inner wall by the sum of the inertial lift force and the Dean drag force, the spacing between these two cell streams was maximized, leading to a higher separation efficiency. However, in a spiral channel on a flat surface, the radius of curvature changes, and this causes continuous changes in its Dean num-

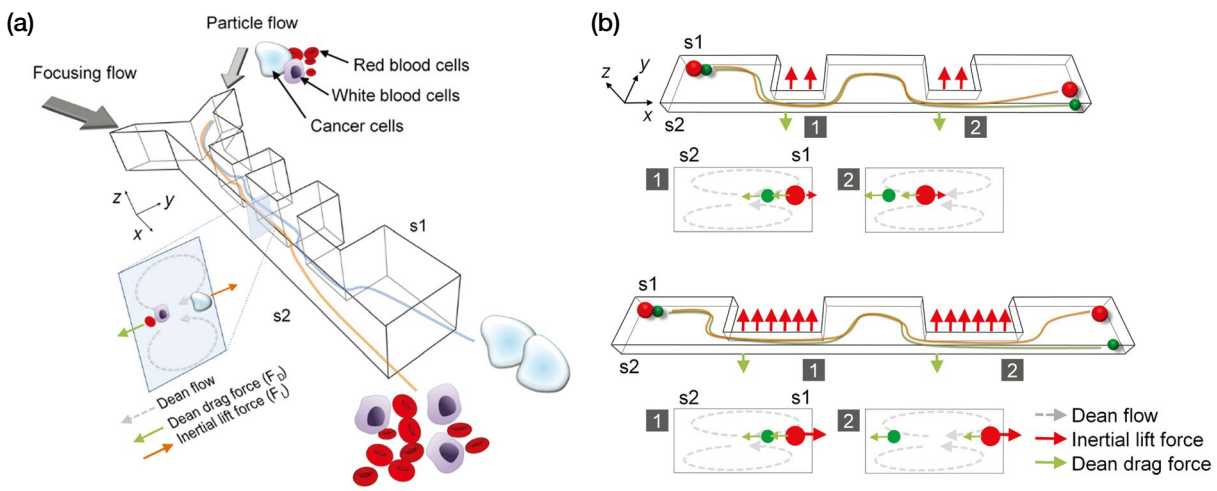

Figure 5. Secondary flow induced in a contraction–expansion arrays (CEA). (a) Schematic of Dean drag force and inertial lift force in a CEA microchannel. The direction of particle migration is determined by balancing the magnitudes of the two forces, which depend on the cell size. Reproduced with permissions[50]. Copyright 2013, American Chemical Society. (b) Modulation of force balance by changing the contraction length in a CEA microchannel. Reproduced with permissions[51]. Copyright 2014, Elsevier.

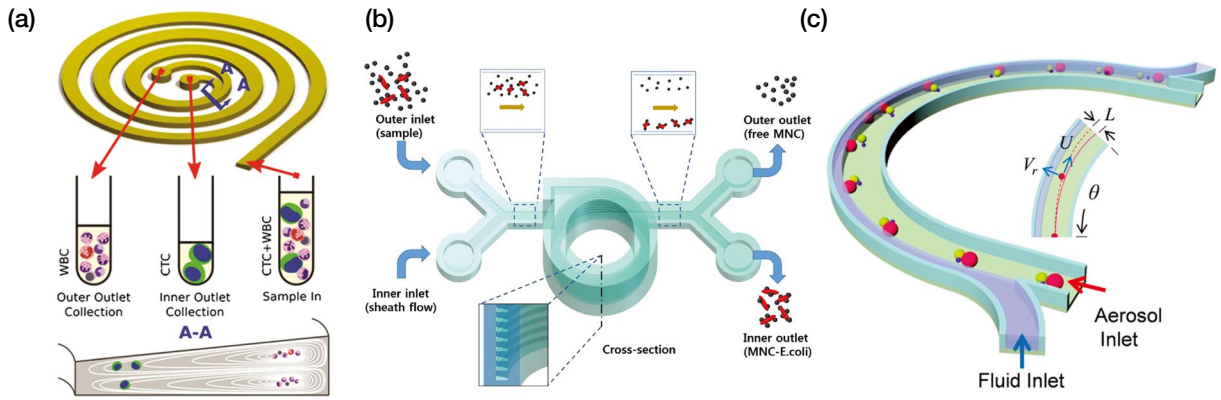

Figure 6. Various applications utilizing spiral channels. (a) A spiral channel with a trapezoidal cross section for the enrichment of extremely rare circulating tumor cells (CTCs) from the blood sample. Reproduced under a Creative Commons license (Attribution-Noncommercial)[55]. (b) Helical trapezoidal microchannels around a cylindrical chamber to sperate magnetic nanoparticle clusters (MNCs) with *E. coli* from free MNCs. Reproduced under a Creative Commons license (Attribution-Noncommercial)[56]. (c) Continuous sampling of *Staphylococcus epidermidis* into liquid phase. Reproduced with permissions[57]. Copyright 2017, American Chemical Society.

ber, which makes it difficult to predict the behavior of flow. To overcome this issue, Lee *et al*. developed a new design that helically piled up these trapezoidal microchannels around a cylindrical chamber, which can offer a constant radius of curvature and compact device size (Figure 6b)[56]. They conducted the separation of magnetic nanoparticle clusters (MNCs) with *Escherichia coli* (*E. coli*) from free MNCs based on the size difference.

This curved channel-based inertial microfluidics can also be further utilized for the detection of bioaerosol. Bioaerosols are airborne particulate matters of biological origin, and they usually have adverse health effects, such as asthma, pneumonia, allergies, and infectious diseases. Since highly concentrated toxic bioaerosols can have a detrimental effect on human health, effective bioaerosol monitoring systems are required. In this regard, Choi *et al*. reported a microfluidic device for the sampling of aerosols into liquids, especially for *Staphylococcus epidermidis* (Figure 6c)[57]. During the fluids flowing through the curved channel, the cells are moved from the air into the liquid phase by the particle centrifugal force and Dean drag force. This device can be used as a simple, portable, and cost-effective airborne microorganism collector for real-time bioaerosol detection.

Potential Novel Inertial Microfluidic Channel Designs for Future Cell Sorting Applications

Recently, unique inertial microfluidic channel designs and integration with various technologies have been newly proposed. Some of these studies have shown the separation of real cells, but most of them were limited to presenting the potential of new technology with artificial microparticles, and there is still a long way to go in terms of separation efficiency. In this section, some novel designs for the future cell sorting applications are introduced.

First, a recent study using isosceles right triangular cross section suggested the potential use of various cross-sectional shapes other than conventional rectangular or circular cross sections as a control parameter for microfluidic cell manipulations (Figure 7a)[58]. As the shape of channel cross section changes, focused particles in the rectangular channel migrate to the top focusing positions of the triangular channel. The larger particles are then aligned along the channel centerline in the downstream rectangular cross section, while the smaller particles are ordered away from the centerline.

Second, asymmetric focusing of particles by introducing the sheath flows with different viscosities can be a new approach (Figure 7b)[59]. In this system, the high-velocity gradient formed by the viscosity difference of the two sheath flows causes the larger particles to migrate away from the original streamline to the side of the higher relative velocity, while the smaller particles remain close to their original streamline.

This concept can be further extended to actively control the number and locations of the focusing positions by tuning the flow rates and viscosities of multiple liquids (Figure 7c)[60]. Passive inertial microfluidic sorting is generally known to be fixed and difficult to adjust, so the passive devices must be designed and optimized for each application, while the same active device can perform

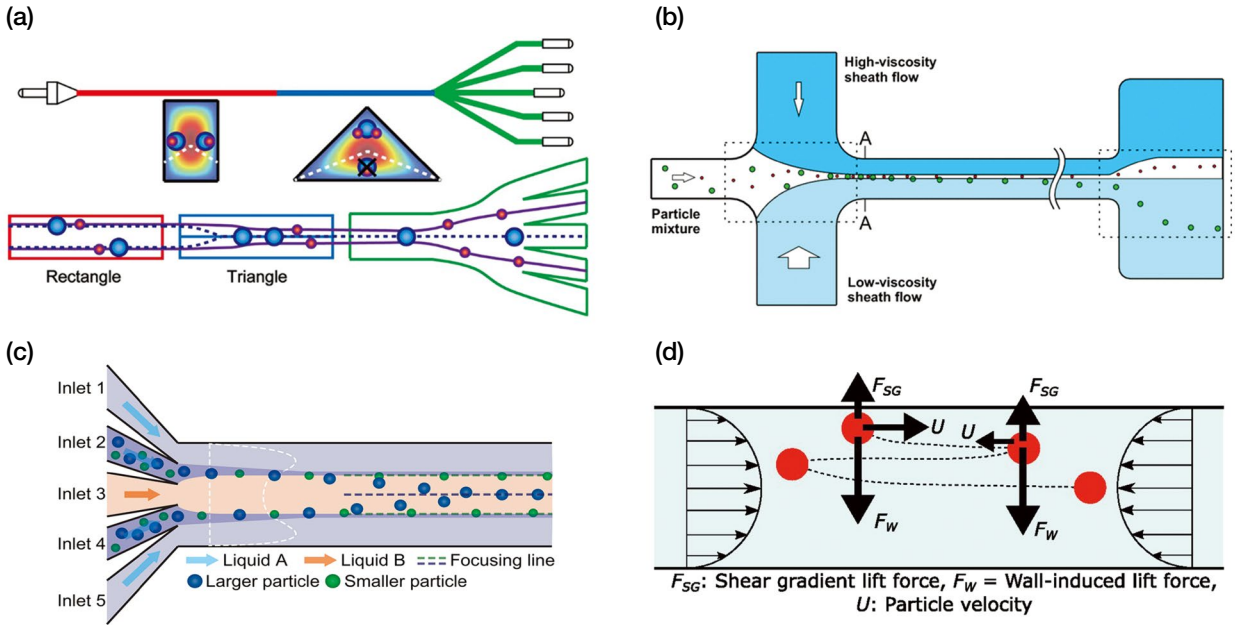

Figure 7. Potential novel inertial microfluidic channel designs for future cell sorting applications. (a) Size-dependent inertial focusing in an isosceles right triangular channel. Reproduced with permissions[58]. Copyright 2018, American Chemical Society. (b) Viscosity-difference-induced asymmetric selective focusing. Reproduced with permissions[59]. Copyright 2016, Springer Nature. (c) Active control of inertial focusing positions and particle separations enabled by velocity profile tuning with coflow systems. Reproduced with permissions[60]. Copyright 2018, American Chemical Society. (d) Oscillatory inertial focusing in infinite microchannels. Reproduced under CC BY-NC-ND or CC BY license[63].

multiple functions. In this sense, the real-time active control of the inertial focusing positions achieved using this coflow system can offer a high degree of freedom in the particle controllability of passive microfluidics.

Lastly, the capabilities of inertial microfluidics are being expanded from larger bioparticles, such as blood cells, CTCs, and stem cells, to micron and submicron particles, such as bacteria and subcellular organelles. Wang *et al*. showed that particles with a diameter of 2 μm and even a submicrometer can be focused to stable equilibrium positions by using a rigid polymer particle with optimized serpentine microchannel geometry[61]. The inertial focusing of 1 μm-sized spherical polystyrene particles and *Escherichia coli* was also demonstrated by utilizing high pressure in a robust glass chip[62]. Furthermore, Toner's group suggested a new idea of oscillatory inertial focusing, which switches the direction of the flow at a high frequency (Figure 7d)[63]. This oscillatory microfluidics can provide "infinite channels" only with a short and fixed channel length by alternating the direction of flow, and the directionality of inertial lift forces acting on the particle is preserved due to the symmetry of the velocity field along the flow axis. Using this technique, they showed the inertial focusing of synthetic particles with a diameter of 500 nm and a submicron bacterium, *Staphylococcus aureus*.

Conclusion

This review provided an overview of inertial microfluidics-based cell sorting. The fundamental dynamics of particle movements has been explained by several forces acting on the particles and their balances. Subsequently, recent developments in inertial microfluidics were introduced according to the structure of microchannels. It could be applied to a wide range of applications from tools for biological experiments to the separation of biomedical samples and environmental monitoring.

Although there have been in-depth studies on the mechanism of inertial microfluidics, the quantitative design rules are still lacking. More dedicated investigations are required to reveal the underlying principles of inertial focusing in various channel designs. Research on the effect of particle shape and deformability as well as particle size will be also meaningful. In addition, more efforts are needed to improve separation efficiency. The serial repetition of purification by the parallelized designs or the optimization of the channel structure can be employed in order to achieve complete separation.

The integration of inertial microfluidics and other active cell sorting technologies might also serve as a good option. Besides, the combination with downstream detection devices, such as optofluidic devices, will also allow the automated particle sorting and identification. The development of cost-effective fabrication methods and the extension to elasto-inertial microfluidics for nano-scale particles are another interesting topics for future works. In conclusion, although significant advances have been achieved in inertial microfluidics over the past few decades, we believe that there are still many areas awaiting exploration and exploitation.

Acknowledgements This research was supported by the National Research Foundation of Korea (NRF) (NRF-2016R1A2B3015986, NRF-2015M3A9B3028685, and NRF-2017M3A7B4039936) funded by the Ministry of Science and ICT.

References

1. Yu, Z.T.F., Yong, K.M.A. & Fu, J. Microfluidic blood cell sorting: now and beyond. *Small* **10**, 1687-1703 (2014).
2. Wyatt Shields IV, C., Reyes, C. & López, G.P. Microfluidic cell sorting: a review of the advances in the separation of cells from debulking to rare cell isolation. *Lab Chip* **15**, 1230-1249 (2015).
3. Antfolk, M. & Laurell, T. Continuous flow microfluidic separation and processing of rare cells and bioparticles found in blood-a review. *Anal. Chim. Acta* **965**, 9-35 (2017).
4. Wu, J., Chen, Q. & Lin, J.-M. Microfluidic technologies in cell isolation and analysis for biomedical applications. *Analyst* **142**, 421-441 (2017).
5. Mao, X., Lin, S.-C.S., Dong, C. & Huang, T.J. Single-layer planar on-chip flow cytometer using microfluidic drifting based three-dimensional (3D) hydrodynamic focusing. *Lab Chip* **9**, 1583-1589 (2009).
6. Lin, S.-C., Yen, P.-W., Peng, C.-C. & Tung, Y.-C. Single channel layer, single sheath-flow inlet microfluidic flow cytometer with three-dimensional hydrodynamic focusing. *Lab Chip* **12**, 3135-3141 (2012).
7. Mach, A.J., Adeyiga, O.B. & Di Carlo, D. Microfluidic sample preparation for diagnostic cytopathology. *Lab Chip* **13**, 1011-1026 (2013).
8. Li, X., Chen, W., Liu, G., Lu, W. & Fu, J. Continuous-flow microfluidic blood cell sorting for unprocessed whole blood using surface-micromachined microfiltration membranes. *Lab Chip* **14**, 2565-2575 (2014).
9. Tripathi, S., Kumar, Y.V.B., Agrawal, A., Prabhakar, A. & Joshi, S.S. Microdevice for plasma separation from whole human blood using bio-physical and geometrical effects. *Sci. Rep.* **6**, 26749 (2016).
10. Myung, J.H. & Hong, S. Microfluidic devices to enrich and isolate circulating tumor cells. *Lab Chip* **15**, 4500-4511 (2015).
11. Yeo, T. *et al.* Microfluidic enrichment for the single cell analysis of circulating tumor cells. *Sci. Rep.* **6**, 22076 (2016).
12. Doh, I. & Cho, Y.-H. A continuous cell separation chip using hydrodynamic dielectrophoresis (DEP) process. *Sens. Actuators A Phys.* **121**, 59-65 (2005). https://doi.org/10.1016/j.sna.2005.01.030
13. Çetin, B. & Li, D. Dielectrophoresis in microfluidics technology. *Electrophoresis* **32**, 2410-2427 (2011).
14. Pamme, N. Continuous flow separations in microfluidic devices. *Lab Chip* **7**, 1644-1659 (2007).
15. Robert, D. *et al.* Cell sorting by endocytotic capacity in a microfluidic magnetophoresis device. *Lab Chip* **11**, 1902-1910 (2011).
16. Shen, F., Hwang, H., Hahn, Y.K. & Park, J.-K. Label-free cell separation using a tunable magnetophoretic repulsion force. *Anal. Chem.* **84**, 3075-3081 (2012).
17. Shi, J., Huang, H., Stratton, Z, Huang, Y. & Huang, T.J. Continuous particle separation in a microfluidic channel via standing surface acoustic waves (SSAW). *Lab Chip* **9**, 3354-3359 (2009).
18. Li, P. *et al.* Acoustic separation of circulating tumor cells. *Proc. Natl. Acad. Sci. U.S.A.* **112**, 4970-4975 (2015).
19. Urbansky, A. *et al.* Rapid and effective enrichment of mononuclear cells from blood using acoustophoresis. *Sci. Rep.* **7**, 17161 (2017).
20. Wang, X. *et al.* Enhanced cell sorting and manipulation with combined optical tweezer and microfluidic chip technologies. *Lab Chip* **11**, 3656-3662 (2011).
21. Landenberger, B., Höfemann, H., Wadle, S. & Rohrbach, A. Microfluidic sorting of arbitrary cells with dynamic optical tweezers. *Lab Chip* **12**, 3177-3183 (2012).
22. Yamada, M., Nakashima, M. & Seki, M. Pinched flow fractionation: Continuous size separation of particles utilizing a laminar flow profile in a pinched microchannel. *Anal. Chem.* **76**, 5465-5471 (2004).
23. Ashley, J.F., Bowman, C.N. & Davis, R.H. Hydrodynamic separation of particles using pinched-flow fractionation. *AIChE J.* **59**, 3444-3457 (2013). https://doi.org/10.1002/aic.14087
24. Huang, L.R., Cox, E.C., Austin, R.H. & Sturm, J.C. Continuous particle separation through deterministic lateral displacement. *Science* **304**, 987-990 (2004).
25. McGrath, J., Jimenez, M. & Bridle, H. Deterministic lateral displacement for particle separation: a review. *Lab Chip* **14**, 4139–4158 (2014).
26. Tran, T.S.H., Ho, B.D., Beech, J.P. & Tegenfeldt, J.O. Open channel deterministic lateral displacement for particle and cell sorting. *Lab Chip* **17**, 3592-3600 (2017).
27. Choi, S. & Park, J.-K. Continuous hydrophoretic sepa-

ration and sizing of microparticles using slanted obstacles in a microchannel. *Lab Chip* **7**, 890-897 (2007).
28. Choi, S., Song, S., Choi, C. & Park, J.-K. Hydrophoretic sorting of micrometer and submicrometer particles using anisotropic microfluidic obstacles. *Anal. Chem.* **81**, 50-55 (2009).
29. Kim, B., Lee, J.K. & Choi, S. Continuous sorting and washing of cancer cells from blood cells by hydrophoresis. *BioChip J.* **10**, 81-87 (2016). https://doi.org/10.1007/s13206-016-0201-0
30. Di Carlo, D. Inertial microfluidics. *Lab Chip* **9**, 3038-3046 (2009).
31. Zhang, J. *et al*. Fundamentals and applications of inertial microfluidics: a review. *Lab Chip* **16**, 10-34 (2016).
32. Godino, N., Jorde, F., Lawlor, D., Jaeger, M. & Duschl, C. Purification of microalgae from bacterial contamination using a disposable inertia-based microfluidic device. *J. Micromech. Microeng.* **25**, 084002 (2015). http://dx.doi.org/10.1088/0960-1317/25/8/084002
33. Di Carlo, D., Irimia, D., Tompkins, R.G. & Toner, M. Continuous inertial focusing, ordering, and separation of particles in microchannels. *Proc. Natl. Acad. Sci. U.S.A.* **104**, 18892-18897 (2007).
34. Bhagat, A.A.S., Kuntaegowdanahalli, S.S. & Papautsky, I. Enhanced particle filtration in straight microchannels using shear-modulated inertial migration. *Phys. Fluids* **20**, 101702 (2008). https://doi.org/10.1063/1.2998844
35. Amini, H., Lee, W. & Di Carlo, D. Inertial microfluidic physics. *Lab Chip* **14**, 2739-2761 (2014).
36. Lee, M.G., Choi, S. & Park, J.-K. Inertial separation in a contractio-expansion array microchannel. *J. Chromatogr. A* **1218**, 4138-4143 (2011).
37. Choi, K. *et al*. Negative selection by spiral inertial microfluidics improves viral recovery and sequencing from blood. *Anal. Chem.* **90**, 4657-4662 (2018).
38. Park, J.-S. & Jung, H.-I. Multiorifice flow fractionation: continuous size-based separation of microspheres using a series of contraction/expansion microchannels. *Anal. Chem.* **81**, 8280-8288 (2009).
39. Segré, G. & Silberberg, A. Radial particle displacements in Poiseuille flow of suspensions. *Nature* **189**, 209-210 (1961). https://doi.org/10.1038/189209a0
40. Segré, G. & Silberberg, A. Behaviour of macroscopic rigid spheres in Poiseuille flow Part 2. Experimental results and interpretation. *J. Fluid Mech.* **14**, 136-157 (1962). https://doi.org/10.1017/S0022112062001111
41. Mach. A.J. & Di Carlo, D. Continuous scalable blood filtration device using inertial microfluidics. *Biotechnol. Bioeng.* **107**, 302-311 (2010).
42. Li, M., van Zee, M., Goda, K. & Di Carlo, D. Size-based sorting of hydrogel droplets using inertial microfluidics. *Lab Chip* **18**, 2575-2582 (2018).
43. Zhou, J., Giridhar, P.V., Kasper, S. & Papautsky, I. Modulation of aspect ratio for complete separation in an inertial microfluidic channel. *Lab Chip* **13**, 1919-1929 (2013).
44. Tan, A.P. *et al*. Continuous-flow cytomorphological staining and analysis. *Lab Chip* **14**, 522-531 (2014).
45. Dudani, J.S., Go, D.E., Gossett, D.R., Tan, A.P. & Di Carlo, D. Mediating millisecond reaction time around particles and cells. *Anal. Chem.* **86**, 1502-1510 (2014).
46. Dudani, J.S. *et al*. Rapid inertial solution exchange for enrichment and flow cytometric detection of microvesicles. *Biomicrofluidics* **9**, 014112 (2015).
47. Shen, S. *et al*. Regulating secondary flow in ultra-low aspect ratio microchannels by dimensional confinement. *Adv. Theory Simul.* **1**, 1700034 (2018). https://doi.org/10.1002/adts.201700034
48. Bhagat, A.A.S., Kuntaegowdanahalli, S.S., Kaval, N., Seliskar, C.J. & Papautsky, I. Inertial microfluidics for sheath-less high-throughput flow cytometry. *Biomed. Microdevices* **12**, 187-195 (2010).
49. Lee, M.G. *et al*. Inertial blood plasma separation in a contraction–expansion array microchannel. *Appl. Phys. Lett.* **98**, 253702 (2011). https://doi.org/10.1063/1.3601745
50. Lee, M.G., Shin, J.H., Bae, C.Y., Choi, S. & Park, J.-K. Label-free cancer cell separation from human whole blood using inertial microfluidics at low shear stress, *Anal. Chem.* **85**, 6213-6218 (2013).
51. Lee, M.G., Shin, J.H., Choi, S. & Park, J.-K. Enhanced blood plasma separation by modulation of inertial lift force. *Sens. Actuators B Chem.* **190**, 311-317 (2014). https://doi.org/10.1016/j.snb.2013.08.092
52. Kuntaegowdanahalli, S.S., Bhagat, A.A.S., Kumar, G. & Papautsky, I. Inertial microfluidics for continuous particle separation in spiral microchannels. *Lab Chip* **9**, 2973-2980 (2009).
53. Zhang, J., Li, W. & Alici, G. Inertial microfluidics: mechanisms and applications. In D. Zhang & B. Wei (Eds.), *Advanced Mechatronics and MEMS Devices II*, 563-593 (2017).
54. Hou, H.W. *et al*. Isolation and retrieval of circulating tumor cells using centrifugal forces. *Sci. Rep.* **3**, 1259 (2013).
55. Warkiani, M.E. *et al*. Slanted spiral microfluidics for the ultra-fast, label-free isolation of circulating tumor cells. *Lab Chip* **14**, 128-137 (2014).
56. Lee, W. *et al*. 3D-printed microfluidic device for the detection of pathogenic bacteria using size-based separation in helical channel with trapezoid cross-section. *Sci. Rep.* **5**, 7717 (2015).
57. Choi, J., Hong, S.C., Kim, W. & Jung, J.H. Highly enriched, controllable, continuous aerosol sampling using inertial microfluidics and its application to real-time detection of airborne bacteria. *ACS Sensors* **2**, 513-521 (2017).
58. Kim, J. *et al*. Size-dependent inertial focusing position shift and particle separations in triangular microchannels. *Anal. Chem.* **90**, 1827-1835 (2018).

59. Xu, W., Hou, Z., Liu, Z. & Wu, Z. Viscosity-difference-induced asymmetric selective focusing for large stroke particle separation. *Microfluid. Nanofluid.* **20**, 128 (2016).
60. Lee, D. *et al.* Active control of inertial focusing positions and particle separations enabled by velocity profile tuning with coflow systems. *Anal. Chem.* **90**, 2902-2911 (2018).
61. Wang, L. & Dandy, D.S. High-throughput inertial focusing of micrometer- and sub-micrometer-sized particles separation. *Adv. Sci.* **4**, 1700153 (2017).
62. Cruz, J. *et al.* High pressure inertial focusing for separating and concentrating bacteria at high throughput. *J. Micromech. Microeng.* **27**, 084001 (2017).
63. Mutlu, B.R., Edd, J.F. & Toner, M. Oscillatory inertial focusing in infinite microchannels. *Proc. Natl. Acad. Sci. U.S.A.* **115**, 7682-7687 (2018).